agriculture

MDPI

Article

Artificial Neural Network Modeling of Greenhouse Tomato Yield and Aerial Dry Matter

Kelvin López-Aguilar [1], Adalberto Benavides-Mendoza [2], Susana González-Morales [3], Antonio Juárez-Maldonado [4], Pamela Chiñas-Sánchez [5] and Alvaro Morelos-Moreno [3,*]

1 Doctorado en Ciencias en Agricultura Protegida, Universidad Autónoma Agraria Antonio Narro, Saltillo 25315, Mexico; uaaan88@hotmail.com
2 Horticultura, Universidad Autónoma Agraria Antonio Narro, Saltillo 25315, Mexico; abenmen@gmail.com
3 CONACYT-Universidad Autónoma Agraria Antonio Narro, Saltillo 25315, Mexico; qfb_sgm@hotmail.com
4 Botánica, Universidad Autónoma Agraria Antonio Narro, Saltillo 25315, Mexico; juma841025@gmail.com
5 Tecnológico Nacional de México, I. T. Saltillo, Saltillo 25280, Mexico; pame.ch.s@gmail.com
* Correspondence: amorelosmo@conacyt.mx; Tel.: +52-844-327-0462

Received: 19 February 2020; Accepted: 24 March 2020; Published: 1 April 2020

Abstract: Non-linear systems, such as biological systems, can be simulated by artificial neural network (ANN) techniques. This research aims to use ANN to simulate the accumulated aerial dry matter (leaf, stem, and fruit) and fresh fruit yield of a tomato crop. Two feed-forward backpropagation ANNs, with three hidden layers, were trained and validated by the Levenberg–Marquardt algorithm for weights and bias adjusted. The input layer consisted of the leaf area, plant height, fruit number, dry matter of leaves, stems and fruits, and the growth degree-days at 136 days after transplanting (DAT); these were obtained from a tomato crop, a hybrid, EL CID F1, with indeterminate growth habits, grown with a mixture of peat moss and perlite 1:1 (*v*/*v*) (substrate) and calcareous soil (soil). Based on the experimentation of the ANNs with one, two and three hidden layers, with MSE values less than 1.55, 0.94 and 0.49, respectively, the ANN with three hidden layers was chosen. The 7-10-7-5-2 and 7-10-8-5-2 topologies showed the best performance for the substrate (R = 0.97, MSE = 0.107, error = 12.06%) and soil (R = 0.94, MSE = 0.049, error = 13.65%), respectively. These topologies correctly simulated the aerial dry matter and the fresh fruit yield of the studied tomato crop.

Keywords: soft computing; simulation model; tomato yield; dry weight; training; validation

1. Introduction

Quantitative interpretations of plant growth through descriptive models have been developed via two mathematical approaches known as classical and functional analysis [1]. ANNs are a nonlinear mapping structure based on the function of the human brain [2], offering learning capabilities. ANNs have been developed to build mathematical models that mimic the computing power of the human brain, with powerful processing capabilities that have been demonstrated in various real-world applications [3]. Agriculture offers many wide applications for ANNs [4–8].

The neuron is the basic working unit of an ANN. This neuron does not have a predefined meaning and evolves during the learning process in a manner that can characterize the target's function [3].

ANNs allow us to develop models based on the intrinsic relations among the variables, without prior knowledge of their functional relationships [9]. Soft computing for ANN techniques has been widely used to develop models to predict different crop indicators, such as growth, yield, and other biophysical processes, and also because of the commercial importance of tomato [10–23] and other vegetables, such as lettuce [24–30], pepper [31–34], cucumber [35–38], wheat [39–45], rice [46–48], oat [49], maize [50,51], corn [52–54], corn and soybean [55], soybean [56], green peas [57], basil [58],

cabbage [59], onion [60], potato [61,62], melon [63], fodder [64], sugar cane [65,66], banana [67,68], orange [69], yacon tuber [70], and jack fruit [71].

Neural networks are models based on emulating human reasoning, which have great advantages in applying mathematical reasoning to situations with unknown relationships between the dependent and independent variables [72]. This research aimed to build two ANNs in order to simulate the aerial dry matter (leaf, stem, and fruit) and fresh fruit yield in a tomato crop grown into two culture systems.

2. Materials and Methods

2.1. Establishment and Growth of Tomato Crop

Seeds of a saladette tomato (*Solanum lycopersicum* L.) hybrid "EL CID F1" with undetermined growth habits were seeded in polystyrene trays. After 35 days, the seedlings were transplanted equidistantly, with 3 plants per square meter, into 8 L black polyethylene containers. Two culture systems were used: substrate and the soil. Tomato plants were grown in a multi-tunnel greenhouse with a polyethylene cover located in the Horticulture Department at the Agricultural University "Antonio Narro" in Saltillo, Mexico (25°21′ N, 101°01′ W, altitude 1743 m). The crop cycle extended from May 20th to November 11th, 2017, with average values of temperature at 21 °C, photosynthetic active radiation of 565 µmol m^{-2} s^{-1}, and relative humidity of 51%. The tomato plants were maintained on a single stem by removing the axillary buds. Fertilization consisted of a Steiner nutrient solution [73] applied three times a day by watering to concentrations of 25%, 50%, 75%, and 100% at the transplanting date and 15, 28, and 35 DAT. The irrigation water was gradually increased during the crop cycle from 0.5 to 3 L per plant per day from the transplanting date to harvesting by using an irrigation system.

2.2. Measuring of ANN Input Values

The input variables consisted of six crop variables: leaf area (LA), plant height (PH), fruit number (FN), dry matter of leaves (LDM), stems (SDM), and fruits (FDM), and the accumulated air temperature (growth degree days) at 136 DAT. Four tomato plants were randomly chosen for the substrate and soil culture systems. The leaf areas of the tomato plants were measured with a portable LI-3100C device (LI-COR®, Inc. Nebraska, USA) as the square centimeters per plant (cm^2 $plant^{-1}$). The plant heights or stem lengths of the tomato plants were measured with a flex meter from the substrate surface through the apical bud in centimeters (cm). The fruit number was registered for each plant. The fresh matter (leaves, stems, and fruits) was measured separately with a digital balance, and the leaves, stems, and fruits were dehydrated separately in a drying oven at 70 °C until obtaining a constant weight, expressed in grams per plant (g $plant^{-1}$). The greenhouse air temperature in Celsius degree (°C) was measured with a WhatchDog 1650 datalogger (Spectrum Technologies Inc., St. Joseph, IN, USA) at a time interval of 15 min. The growth degree-days (GDD) were computed according to the residual method [74] in Excel with Equation (1):

$$GDD = \sum_{i=1}^{n} (T_i - T_b), \quad T_i = \frac{T_{min} + T_{max}}{2} \tag{1}$$

where GDD is the growth degree-day on the ith day from the transplanting date to 136 DAT (°D), T_i is the mean greenhouse air temperature on the ith day (°C), T_b is the base temperature at which the growth ceased (for the tomato grown under greenhouse conditions T_b = 10 °C [75]), and T_{min} and T_{max} are, respectively, the minimum and maximum daily temperatures (°C).

The plant development rate is proportional to $Ti - Tb$, which implies that the development stage will be proportional to the integrated temperature $\int (Ti - Tb)dt$, where the plant development rate ceases when $Ti - Tb < Tb$ [76].

2.3. Artificial Neural Networks

Two feed-forward backpropagation ANNs with an input layer, three hidden layers, and two output layers were trained and validated by the Levenberg–Marquardt algorithm for adjusted weights and bias [77–79]. The input layer consisted of seven neurons with the average values of five replications of the leaf area (LA), plant height (PH), fruit number (FN), dry matter of leaves (LDM), stems (SDM) and fruits (FDM), and growth degree days (GDD) from the accumulated greenhouse air temperature over the crop cycle. The output layers consisted of the fresh fruit yield and aerial dry matter. Different ANN topology arrays, varying the neuron number in the three hidden layers, were evaluated in order to determine the appropriated network topology to be used in each cropping system. The 10-7-5 and 10-8-5 topologies were used at the hidden layers for the substrate and soil, respectively, according to their data and learning rates. The input and output data were normalized by the Min–Max method [80,81] in the RStudio software [82], where the data were randomly divided into three sets: training 70%, validation 15%, and testing 15%, according to the literature, where these percentages were used for the data [64,83].

2.4. Neuron Topologies in the Hidden Layers

Neuron numbers between 5 to 10, 4 to 10, and 1 to 5 were randomly chosen in the three hidden layers in order to build different topology arrays [64] (Table 1). In most applications, the neuron number is determined by trial and error [84]. The different topology arrays resulting from these combinations were evaluated in the MATLAB neural network toolbox [85], and the following transfer functions were used: tangent sigmoidal hyperbolic (tansig), logarithmic sigmoidal hyperbolic (logsig), and pure lineal (purelin) [85,86], with a learning rate of 0.5 [63], 1000 epochs [64], minimum performance gradient of $1e^{-07}$ and adaptation value of 0.001. The tangent sigmoidal hyperbolic (tansig) transfer function presented the best performance in the hidden layers, and the pure lineal (purelin) transfer function presented the best performance in the output layers, defined by its lower mean square error (MSE) values for the substrate and soil (Table 1).

Table 1. Mean square error (MSE) of the evaluated hidden layers topologies for the substrate and soil.

Hidden Layers	Culture System	Hidden Layer			Transfer Functions		Epochs	MSE
		1st	2nd	3rd	Hidden Layers	Output Layer		
1	Substrate	10	-	-	Logsig	Logsig	12	0.238
		10	-	-	Logsig	Purelin	8	0.136
		10	-	-	Logsig	Tansig	13	0.257
		10	-	-	Purelin	Purelin	4	1.25
		10	-	-	Purelin	Logsig	9	0.204
		10	-	-	Purelin	Tansig	9	0.221
		10	-	-	Tansig	Tansig	11	0.15
		10	-	-	Tansig	Logsig	8	0.572
		10	-	-	Tansig	Purelin	8	0.341
	Soil	10	-	-	Logsig	Logsig	10	0.141
		10	-	-	Logsig	Purelin	10	0.253
		10	-	-	Logsig	Tansig	19	0.54
		10	-	-	Purelin	Purelin	4	1.55
		10	-	-	Purelin	Logsig	10	0.413
		10	-	-	Purelin	Tansig	9	0.154
		10	-	-	Tansig	Tansig	18	0.261
		10	-	-	Tansig	Logsig	63	0.119
		10	-	-	Tansig	Purelin	7	0.382

Table 1. *Cont.*

Hidden Layers	Culture System	Hidden Layer 1st	2nd	3rd	Transfer Functions Hidden Layers	Output Layer	Epochs	MSE
2	Substrate	10	5	-	Logsig	Logsig	8	0.128
		10	6	-	Logsig	Logsig	9	0.372
		10	7	-	Logsig	Logsig	7	0.114
		10	8	-	Logsig	Logsig	6	0.253
		10	9	-	Logsig	Logsig	7	0.217
		10	5	-	Logsig	Purelin	6	0.382
		10	6	-	Logsig	Purelin	7	0.781
		10	7	-	Logsig	Purelin	6	0.715
		10	8	-	Logsig	Purelin	7	0.566
		10	9	-	Logsig	Purelin	8	0.938
		10	5	-	Logsig	Tansig	6	0.226
		10	6	-	Logsig	Tansig	7	0.217
		10	7	-	Logsig	Tansig	6	0.288
		10	8	-	Logsig	Tansig	6	0.274
		10	9	-	Logsig	Tansig	6	0.2
	Soil	10	5	-	Logsig	Logsig	11	0.262
		10	6	-	Logsig	Logsig	53	0.148
		10	7	-	Logsig	Logsig	7	0.463
		10	8	-	Logsig	Logsig	6	0.186
		10	9	-	Logsig	Logsig	9	0.0986
		10	5	-	Logsig	Purelin	7	0.229
		10	6	-	Logsig	Purelin	6	0.0935
		10	7	-	Logsig	Purelin	7	0.0825
		10	8	-	Logsig	Purelin	7	0.381
		10	9	-	Logsig	Purelin	6	0.0864
		10	5	-	Logsig	Tansig	6	0.234
		10	6	-	Logsig	Tansig	7	0.499
		10	7	-	Logsig	Tansig	16	0.0854
		10	8	-	Logsig	Tansig	6	0.265
		10	9	-	Logsig	Tansig	9	0.199
3	Substrate	5	4	0	Tansig	Tansig	12	0.194
		5	8	8	Tansig	Tansig	11	0.153
		6	7	8	Tansig	Tansig	10	0.164
		10	7	5	Tansig	Purelin	8	0.107
		10	10	5	Tansig	Tansig	11	0.130
		10	8	6	Purelin	Logsig	6	0.311
		10	7	9	Purelin	Tansig	10	0.322
		10	6	5	Purelin	Purelin	4	0.381
		6	9	4	Purelin	Logsig	10	0.232
		9	11	5	Purelin	Tansig	19	0.376
		8	5	7	Logsig	Tansig	15	0.289
		9	10	4	Logsig	Purelin	17	0.379
		9	8	7	Logsig	Purelin	21	0.275
		5	9	6	Logsig	Logsig	9	0.297
		7	8	5	Logsig	Tansig	15	0.327
	Soil	5	4	0	Tansig	Tansig	12	0.323
		8	5	3	Tansig	Purelin	12	0.370
		10	10	5	Tansig	Tansig	13	0.375
		5	7	5	Tansig	Tansig	17	0.260
		10	8	5	Tansig	Purelin	6	0.049
		10	8	7	Purelin	tansig	17	0.276
		6	7	5	Purelin	logsig	4	0.388
		9	6	4	Purelin	Purelin	6	0.391
		7	8	6	Purelin	Logsig	9	0.321
		6	9	8	Purelin	Tansig	7	0.286
		10	7	8	Logsig	Purelin	10	0.389
		8	9	7	Logsig	Tansig	12	0.275
		7	9	8	Logsig	Logsig	16	0.432
		9	8	6	Logsig	Purelin	22	0.488
		6	10	5	Logsig	Tansig	11	0.322

For the hidden layers, the sigmoid hyperbolic tangent (tansig) transfer function (Equation (2)) was used [87]:

$$Y_j = \frac{e^{X_j} - e^{-X_j}}{e^{X_j} + e^{-X_j}} \quad (2)$$

For the output layer, the linear (purelin) transfer function (Equation (3)) was used [87]:

$$Y_j = X_j, \;\; X_j = \sum_{i=1}^{m} W_{ij} Y_i + b_j \quad (3)$$

where m is the number of neurons in the output layer, W_{ij} is the weight of connections between layers i and j, Y_i is the output of the neurons in layer i, and b_j is the bias of the neurons in layer j.

Correlation and dependence are statistical relationships between two or more random variables or observed data values. Correlation refers to any departure of two or more random variables from independence and indicates a relationship between the mean values, thereby offering predictive relationship that can be used in practice. Dependence indicates if the random variables satisfy a mathematical condition of probabilistic independence [88]. The MSE and correlation coefficient (R) were used in this research.

ANN validation was performed in the Matlab 2017a software through the MSE computing (Equation (4)), according to [89]:

$$MSE = \frac{\sum_{j=0}^{P} \sum_{i=0}^{N} \left(d_{ij} - y_{ij}\right)^2}{NP} \quad (4)$$

where P is the number of output neurons, N is the number of exemplars in the dataset, and y_{ij} and d_{ij} are the network output and desired output for exemplar i at processing element j.

Although the *MSE* values indicate the difference between the predicted and experimental values, the *MSE* criterion does not determine their direction, so the R was also calculated with Equation (5), according to [87,89]:

$$R = \frac{\sum_i \left(X_i - \overline{X}\right)\left(d_i - \overline{d}\right)}{N} \Bigg/ \sqrt{\frac{\sum_i \left(d_i - \overline{d}\right)^2}{N} \sqrt{\frac{\sum_i \left(X_i - \overline{X}\right)^2}{N}}} \quad (5)$$

where Xi is the network output, $\overline{X}$ is the mean of the network outputs, d_i is the desired output, $\overline{d}$ is the mean of the desired outputs, and N is the number of exemplars in the dataset.

The performance indicators for building the ANN model included the higher R [90] and the lower *MSE* [66,70].

3. Results

3.1. ANN Topologies

Two feed-forward backpropagation ANNs with an input layer, three hidden layers, and two output layers, were trained and validated by the Levenberg–Marquardt algorithm for adjusted weights and bias. The ANN array with three hidden layers was chosen from the minimum MSE values obtained in the experimentation, which increased until 1.55, 0.94 and 0.49 in the ANN with 1, 2 and 3 hidden layers, respectively (Table 1).

Based on the evaluation of the transfer functions, an ANN with a 10-7-5 topology in the hidden layers was built for the substrate culture system (Figure 1a). This ANN showed the best performance (R = 0.97 and MSE = 0.107), with *tansig* and *purelin* transfer functions in the hidden layers and output layer, respectively (Table 1), while the ANN with a 10-8-5 topology in the hidden layers was built for

the soil culture system (Figure 1b), which showed better performance (R = 0.95 and MSE = 0.049) with *tansig* and *purelin* transfer functions in the hidden layers and output layer, respectively (Table 1).

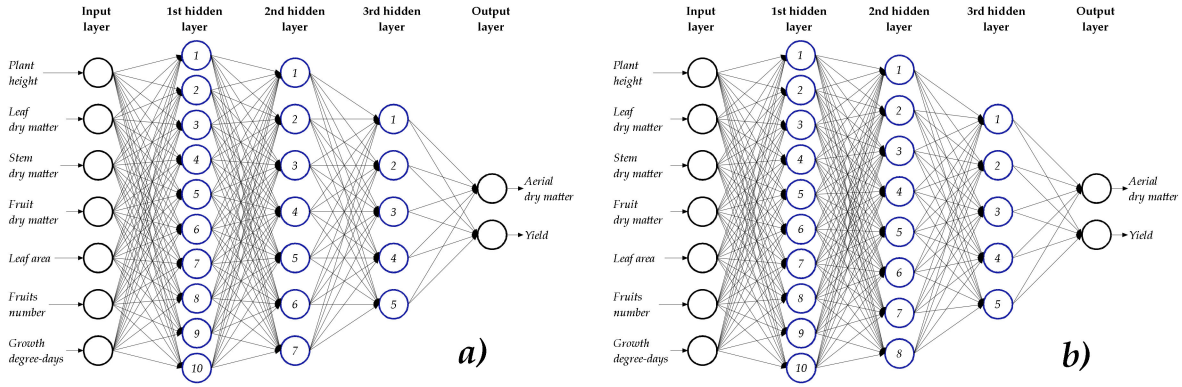

Figure 1. ANN schemes with (**a**) a 7-10-7-5-2 topology for the substrate, and (**b**) a 7-10-8-5-2 topology for the soil.

3.2. Training, Validation, and Test Processes of the ANNs

The training, validation, and test processes were performed with the observed and simulated data for the aerial dry matter and fresh fruit yield of the tomato grown in the substrate (Figure 2a) and soil (Figure 2b) culture systems. All evaluation processes showed R values higher than 0.96 for the substrate and higher than 0.94 for the soil.

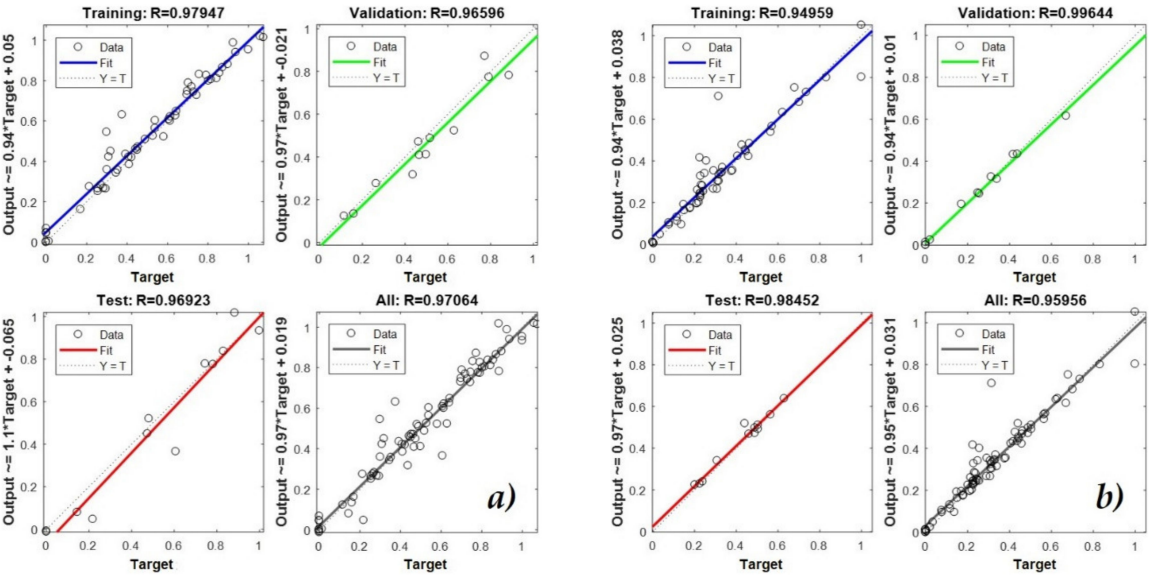

Figure 2. Training, validation, and test processes for the ANNs of the (**a**) substrate, and (**b**) soil.

3.3. Aerial Dry Matter

The observed and simulated data of aerial dry matter over the crop cycle showed R values higher than 0.96 in the substrate (Figure 3a) and higher than 0.98 in the soil (Figure 3b) culture systems. At 136 DAT, the simulated data were underestimated with respect to the observed data because the regression line (black line) was located below the 1–1 line (gray line) for both the substrate and the soil culture systems.

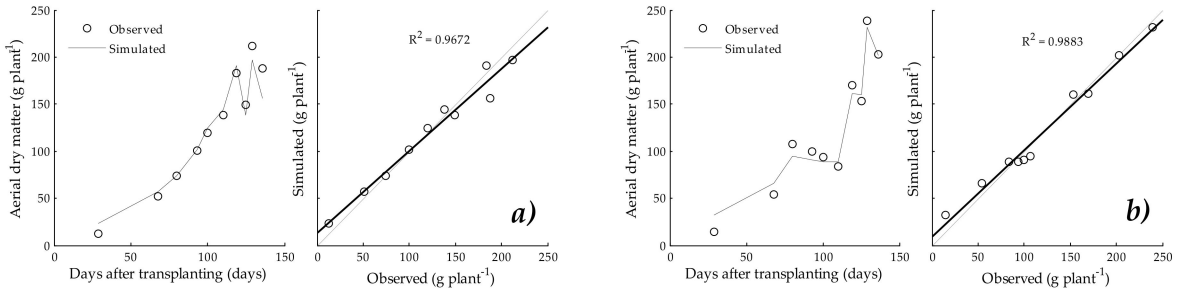

Figure 3. Aerial dry matter of the tomato plants grown in the (**a**) substrate and (**b**) soil.

3.4. Fresh Fruit Yield

The observed and simulated data for the fresh fruit yield over the crop cycle showed R values higher than 0.98 in the substrate (Figure 4a) and higher than 0.97 in the soil (Figure 4b) culture systems. At 136 DAT, the simulated data were overestimated with respect to the observed data because the regression line (black line) was located above the 1–1 line (gray line) for both the substrate and the soil culture systems.

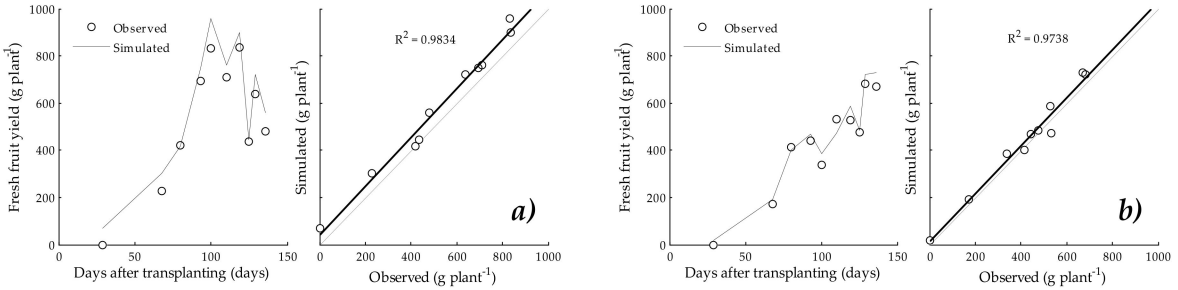

Figure 4. Fresh fruit yield of tomato plants grown in the (**a**) substrate and (**b**) soil.

4. Discussion

According to the evaluation, two neural network architectures were obtained, one for the substrate (7-10-7-5-2) and the other for the soil culture systems (7-10-8-5-2). These architectures showed the best performance and were appropriate according to Gutiérrez [90], who mentioned that the correlation coefficient measures the intensity of the relationship between two variables (X and Y), to justify the inclusion of the comparison criterion and a low value of the MSE. The MSE is calculated by dividing the sum of the squares of the difference of the target value with the value calculated by the neural network, by the total number of data. The MSE value and the training algorithm will allow one to perform an acceptable training to adjust the weights and bias according to the real data [23]. The MSE was used to measure the efficiency of the training process, as mentioned in [66,70].

4.1. ANN Topologies

Two feed-forward backpropagation ANNs were trained and validated by the Levenberg–Marquardt algorithm for weights and bias adjusted, one for substrate and other for soil culture systems. The tansig–purelin transfer functions in the hidden and output layers, respectively, for the two ANNs were used. The ANN outputs were the aerial dry matter and the fresh fruit yield of the tomato grown for the two culture systems.

The ANN with three hidden layers showed a better fit, corresponding to lower MSE values in the two culture systems, with substrate topologies of 10, 7, and 5 neurons in the first, second, and third hidden layers, respectively, and soil topologies of 10, 8, and 5 neurons in the first, second, and third hidden layers, respectively. The topologies of the two culture systems were different only in the second hidden layer, with the soil data higher in one neuron compared to the substrate data. In this

research the tansig, logsig and pureline transfer functions were used, both in the hidden layers and in the output layer, while [91] only used the tansig transfer function in the hidden layers and the pureline transfer function in the output layer.

According to [92], if sigmoidal neurons are used in the output layer, the network output is limited to a very small range; on the other hand, when using a linear neuron, the output can take any value.

The study in [93] used the multilayer perceptron model with the hyperbolic tangent activation function (tansig) for the hidden layers; this study also used the linear function (purelin) in the construction of its topology for the output layer, which was used for the functions of the two networks to simulate the fruit yield and aerial partial biomass in the substrate and soil. The work in [94] used a backpropagation ANN to simulate the photosynthesis rate of tomato plants, a tangent sigmoidal hyperbolic (tansig–logsig) transfer function for the hidden layers, and a linear (purelin) transfer function for the output layer, with the same transfer functions used for the two models in the present study.

4.2. Training, Validation, and Test Processes of the ANNs

Figure 2 shows the correlation between the observed and simulated values for the training, validation, and test data with better performance—that is, the data with $R > 0.96$ (MSE = 0.107) for the substrate and $R > 0.94$ (MSE = 0.049) for the soil culture systems. The objective of this validation is to establish the credibility of a model for a specific purpose, which is usually done through a comparative analysis [95].

The learning rate of 0.5 used in this research for the substrate and the soil culture systems is similar to the learning rate (0.6) used in [63] and is in the range of the recommended values (0.05 to 0.5 [96], 0.1 to 0.7 [97], and 0.05 to 0.75 [98]), where the learning rate value has no influence on the ANN error [97].

The ANN frames with the Levenberg–Marquardt algorithm applied to the multilayer perceptron topology without connections across layers feature topologies that are far from optimal [77], similar to those used in this research. The obtained R used to measure the performance of the network for validation and testing of the data from the tomato crop grown in the substrate were higher than those obtained in [18], which used a dynamic neural network to predict the tomato yield in a semi-closed greenhouse. In the soil data validation, the R (0.99) was similar to that reported in [64], which used an ANN to predict the yield indexes and quality of the three grasses.

During the training, validation, and test processes of the ANNs, the 1–1 line (dashed line) was used to represent a perfect fit if the network output was the same as the desired output. A continuous line represents the best linear fit regression between the observed output data and the simulated output data from the network. It was also observed that increasing the layers did not decrease the MSE, which began to remain constant at 10, 7, and 5 neurons in the hidden layers, with eight epochs for the substrate and 10, 8, and 5 neurons in the hidden layers, with six epochs for the soil. The study in [63] evaluated a three-layer ANN with different neurons in the hidden layer and determined different changes in the mean prediction error as the topology increased—that is, a reduction from 3.34% to 2.21% (9-1-1 to 9-5-1), and an increment from 2.21% to 2.56% (9-5-1 to 9-9-1).

The authors in [99] concluded that the number of hidden layers and the number of neurons must be chosen by the designer and that there is no rule that can determine the optimal number of hidden neurons to solve a given problem. In most applications, determination of the epoch and neuron number is determined by trial and error [84].

4.3. Aerial Dry Matter and Fresh Fruit Yield

This research aimed to use soft computing techniques to model tomato growth. However, the ANN topologies for the substrate and soil culture systems were trained, validated, and tested using the neuron values of the input layers containing the scalar values of the data corresponding to 136 DAT, not with the vectors across the entire crop cycle. The simulated data were well fitted to the observed data in both the substrate and the soil culture systems, with R higher than 0.96 for the aerial dry matter and higher than 0.97 for the fresh fruit yield.

5. Conclusions

The employed feed-forward backpropagation ANNs with 7-10-7-5-2 and 7-10-8-5-2 topologies for the substrate and soil culture systems, respectively, and trained and validated by the Levenberg–Marquardt algorithm for weights and bias adjusted, satisfactory simulated the aerial dry matter and the fresh fruit yield compared to the observed values.

As mentioned earlier, in recent years, soft computing techniques, such as ANNs, have been used to analyze, model, predict, and execute real processes. In real processes, there is variability and uncertainty that, in some situations, cannot be evaluated with traditional mathematical models. Therefore, this paper was focused on the use of different ANN feedforward topologies capable of learning and simulating the cumulative aerial dry matter and yield of the fresh fruit from a tomato crop grown under greenhouse conditions in substrate and soil culture systems.

Based on the data obtained from the tomato crop grown in the substrate and soil, the two designed ANN structures represent a reliable and precise alternative for modelling and simulating the cumulative yield of tomato crops cultivated under different greenhouse conditions, giving average relative errors of 12.06% and 13.65% for the substrate and soil conditions and a R greater than 94% in both cases. The training process for the ANN structures ended before 10 iterations, reaching a MSE of 0.107 for the substrate and a MSE of 0.049 for the soil. These results show the ability to generalize the designed networks. The results indicate that using databases containing 280 data from four plants (four replicates), 10 samples, and seven input variables allowed the networks, during training, to learn the relationships between the studied inputs and outputs. Likewise, these results indicate that soft computing techniques are suitable for the analysis of data with variability, uncertainty, and various correlations, as shown by the tomato crop data.

Author Contributions: Conceptualization, A.M.-M.; methodology, P.C.-S.; software, K.L.-A.; investigation, S.G.-M. and A.J.-M.; data curation, A.M.-M. and A.B.-M.; visualization, A.M.-M.; writing—original draft preparation, K.L.-A.; writing—review and editing, K.L.-A., A.B.-M., S.G.-M., A.J.-M., P.C.-S. and A.M.-M. All authors have read and agreed to the published version of the manuscript.

Funding: This research received no external funding.

Acknowledgments: The authors would like to thank the Cátedras CONACYT program of the CONACYT (National Council of Science and Technology), project number 1426, for its valuable support with greenhouse, climate sensors and laboratory instruments. KLA received a doctoral scholarship from CONACYT, number 618276.

Conflicts of Interest: The authors declare no conflict of interest.

References

1. Hunt, R. Growth analysis, individual plants. In *Encyclopedia of Applied Plant Sciences*; Thomas, B., Murphy, D.J., Murray, B.G., Eds.; Academic Press: London, UK, 2003; pp. 588–596.
2. Lek, S.; Park, Y.S. Artificial Neural Networks. In *Encyclopedia of Ecology*; Jørgensen, S.E., Fath, B.D., Eds.; Academic Press: London, UK, 2008; pp. 237–245.
3. Tripathi, B.K. *High Dimensional Neurocomputing—Growth, Appraisal and Applications*; Springer: Berlin/Heidelberg, Germany, 2015.
4. Jeeva, C.; Shoba, S.A. An efficient modelling agricultural production using artificial neural network (ANN). *Int. Res. J. Eng. Technol.* **2016**, *3*, 3296–3303.
5. Jiménez, D.; Pérez-Uribe, A.; Satizábal, H.; Barreto, M.; van Damme, P.; Tomassini, M. A Survey of Artificial Neural Network-Based Modeling in Agroecology. In *Soft Computing Applications in Industry*; Prasad, B., Ed.; Springer: Berlin/Heidelberg, Germany, 2008; Volume 226, pp. 247–269.
6. Seginer, I. Some artificial neural network applications to greenhouse environmental control. *Comput. Electron. Agric.* **1997**, *18*, 167–186. [CrossRef]
7. Schultz, A.; Wieland, R. The use of neural networks in agroecological modelling. *Comput. Electron. Agric.* **1997**, *18*, 73–90. [CrossRef]
8. Hashimoto, Y. Applications of artificial neural networks and genetic algorithms to agricultural systems. *Comput. Electron. Agric.* **1997**, *18*, 71–72. [CrossRef]

9. Zupan, J.; Gasteiger, J. *Neural Networks in Chemistry and Drug Design*, 2nd ed.; Wiley & Sons, Inc.: New York, NY, USA, 1999.
10. Istiadi, A.; Sulistiyanti, S.R.; Fitriawan, H. Model Design of Tomato Sorting Machine Based on Artificial Neural Network Method using Node MCU Version 1.0. *J. Phys. Conf. Ser.* **2019**, *1376*, 12–26. [CrossRef]
11. Wang, Q.; Qi, F.; Sun, M.; Qu, J.; Xue, J. Identification of Tomato Disease Types and Detection of Infected Areas Based on Deep Convolutional Neural Networks and Object Detection Techniques. *Comput. Intell. Neurosci.* **2019**, *2019*, 1–15. [CrossRef]
12. Fuentes, A.F.; Yoon, S.; Lee, J.; Park, D.S. High-Performance Deep Neural Network-Based Tomato Plant Diseases and Pests Diagnosis System with Refinement Filter Bank. *Front. Plant Sci.* **2018**, *9*, 1162. [CrossRef]
13. Karami, R.; Kamgar, S.; Karparvarfard, S.; Rasul, M.; Khan, M. Biodiesel production from tomato seed and its engine emission test and simulation using Artificial Neural Network. *J. Oil Gas Petrochem. Technol.* **2018**, *5*, 41–62.
14. Suryawati, E.; Sustika, R.; Yuwana, R.S.; Subekti, A.; Pardede, H.F. Deep Structured Convolutional Neural Network for Tomato Diseases Detection. In Proceedings of the 2018 International Conference on Advanced Computer Science and Information Systems, Yogyakarta, Indonesia, 27–28 October 2018; pp. 385–390.
15. Tm, P.; Pranathi, A.; SaiAshritha, K.; Chittaragi, N.B.; Koolagudi, S.G. Tomato Leaf Disease Detection using Convolutional Neural Networks. In In Proceedings of the 2018 Eleventh International Conference on Contemporary Computing, Noida, India, 2–4 August 2018; pp. 1–5.
16. Pedrosa-Alves, D.; Simões-Tomaz, R.; Bruno-Soares, L.; Dias-Freitas, R.; Fonseca-e Silva, F.; Damião-Cruz, C.; Nick, C.; Henriques-da Silva, D.J. Artificial neural network for prediction of the area under the disease progress curve of tomato late blight. *Sci. Agric.* **2017**, *74*, 51–59. [CrossRef]
17. Küçükönder, H.; Boyaci, S.; Akyüz, A. A modeling study with an artificial neural network: Developing estimation models for the tomato plant leaf area. *Turk. J. Agric. For.* **2016**, *40*, 203–212. [CrossRef]
18. Salazar, R.; López, I.; Rojano, A.; Schmidt, U.; Dannehl, D. Tomato yield prediction in a semi-closed greenhouse. *Acta Hortic.* **2015**, *1107*, 263–270. [CrossRef]
19. Ehret, D.L.; Hill, B.D.; Helmer, T.; Edwards, D.R. Neural network modeling of greenhouse tomato yield, growth and water use from automated crop monitoring data. *Comput. Electron. Agric.* **2011**, *79*, 82–89. [CrossRef]
20. Fang, J.; Zhang, C.; Wang, S. Application of Genetic Algorithm (GA) Trained Artificial Neural Network to Identify Tomatoes with Physiological Diseases. In *The International Federation for Information Processing, Proceedings of the CCTA 2007 Computer and Computing Technologies in Agriculture, Wuyishan, China, 18–20 August 2007*; Li, D., Ed.; Springer: Boston, MA, USA, 2008; pp. 1103–1111.
21. Wang, X.; Zhang, M.; Zhu, J.; Geng, S. Spectral prediction of Phytophthora infestans infection on tomatoes using artificial neural network (ANN). *Int. J. Remote Sens.* **2008**, *29*, 1693–1706. [CrossRef]
22. Movagharnejad, K.; Nikzad, M. Modelling of tomato drying using Artificial Neural Network. *Comput. Electron. Agric.* **2007**, *59*, 78–85. [CrossRef]
23. Poonnoy, P.; Tansakul, A.; Chinnan, M. Artificial Neural Network Modeling for Temperature and Moisture Content Prediction in Tomato Slices Undergoing Microwawe-Vacuum Drying. *J. Food Sci.* **2007**, *72*, 42–47. [CrossRef]
24. Karadžić Banjac, M.Ž.; Kovačević, S.Z.; Jevrić, L.R.; Podunavac-Kuzmanović, S.; Tepić Horeck, A.; Vidović, S.; Šumić, Z.; Ilin, Ž.; Adamović, B.; Kuljanin, T. Artificial neural network modeling of the antioxidant activity of lettuce submitted to different postharvest conditions. *J. Food Process. Preserv.* **2019**, *43*, 1–9. [CrossRef]
25. Osco, L.P.; Ramos, A.P.M.; Moriya, É.A.S.; Bavaresco, L.G.; Lima, B.C.; Estrabis, N.; Pereira, D.R.; Creste, J.E.; Júnior, J.M.; Gonçalves, W.N.; et al. Modeling Hyperspectral Response of Water-Stress Induced Lettuce Plants using Artificial Neural Networks. *Remote Sens.* **2019**, *11*, 2797. [CrossRef]
26. Valenzuela, I.C.; Puno, J.C.V.; Bandala, A.A.; Baldovino, R.G.; de Luna, R.G.; De Ocampo, A.L.; Cuello, J.; Dadios, E.P. Quality assessment of lettuce using artificial neural network. In Proceedings of the 2017 IEEE 9th International Conference on Humanoid, Nanotechnology, Information Technology, Communication and Control, Environment and Management, Manila, Philippines, 1–3 December 2017; pp. 1–5.
27. Mistico-Azevedo, A.; de Andrade-Júnior, V.C.; Pedrosa, C.E.; Mattes-de Oliveira, C.; Silva-Dornas, M.F.; Damião-Cruz, C.; Ribeiro-Valadares, N. Application of artificial neural networks in indirect selection: A case study on the breeding of lettuce. *Bragantia* **2015**, *74*, 387–393. [CrossRef]

28. Sun, J.; Dong, L.; Jin, X.M.; Fang, M.; Zhang, M.X.; Lv, W.X. Identification of Pesticide Residues of Lettuce Leaves Based on LVQ Neural Network. *Adv. Mater. Res.* **2013**, *756–759*, 2059–2063. [CrossRef]
29. Lin, W.C.; Block, G. Neural network modeling to predict shelf life of greenhouse lettuce. *Algorithms* **2009**, *2*, 623–637. [CrossRef]
30. Zaidi, M.A.; Murase, H.; Honami, N. Neural Network Model for the Evaluation of Lettuce Plant Growth. *J. Agric. Eng. Res.* **1999**, *74*, 237–242. [CrossRef]
31. Lee, J.W. Growth Estimation of Hydroponically-grown Bell Pepper (*Capsicum annuum* L.) Using Recurrent Neural Network Through Nondestructive Measurement of Leaf Area Index and Fresh Weight. Ph.D. Thesis, Seoul National University, Seoul Korea, August 2019; p. 163.
32. Manoochehr, G.; Fathollah, N. Fruit yield prediction of pepper using artificial neural network. *Sci. Hortic.* **2019**, *250*, 249–253.
33. Figueredo-Ávila, G.; Ballesteros-Ricaurte, J. Identificación del estado de madurez de las frutas con redes neuronales artificiales, una revisión. *Cienc. Agric.* **2016**, *13*, 117–132. [CrossRef]
34. Lin, W.C.; Hill, B.D. Neural network modelling to predict weekly yields of sweet peppers in a commercial greenhouse. *Can. J. Plant Sci.* **2008**, *88*, 531–536. [CrossRef]
35. Lin, K.; Gong, L.; Huang, Y.; Liu, C.; Pan, J. Deep Learning-Based Segmentation and Quantification of Cucumber Powdery Mildew Using Convolutional Neural Network. *Front. Plant Sci.* **2019**, *10*, 155. [CrossRef] [PubMed]
36. Zhang, S.; Zhang, S.; Zhang, C.; Wang, X.; Shi, Y. Cucumber leaf disease identification with global pooling dilated convolutional neural network. *Comput. Electron. Agric.* **2019**, *162*, 422–430. [CrossRef]
37. Pawar, P.; Turkar, V.; Patil, P. Cucumber disease detection using artificial neural network. In Proceedings of the 2016 International Conference on Inventive Computation Technologies, Coimbatore, India 26–27 August 2016; pp. 1–5.
38. Vakilian, K.A.; Massah, J. An artificial neural network approach to identify fungal diseases of cucumber (*Cucumis sativus* L.) plants using digital image processing. *Arch. Phytopathol. Plant Prot.* **2013**, *46*, 1580–1588. [CrossRef]
39. Haider, S.A.; Naqvi, S.R.; Akram, T.; Umar, G.A.; Shahzad, A.; Sial, M.R.; Khaliq, S.; Kamran, M. LSTM Neural Network Based Forecasting Model for Wheat Production in Pakistan. *Agronomy* **2019**, *9*, 72. [CrossRef]
40. Beres, B.L.; Hill, B.D.; Cárcamo, H.A.; Knodel, J.J.; Weaver, D.K.; Cuthbert, R.D. An artificial neural network model to predict wheat stem sawfly cutting in solid-stemmed wheat cultivars. *Can. J. Plant Sci.* **2017**, *97*, 329–336. [CrossRef]
41. Ghodsi, R.; Yani, R.M.; Jalali, R.; Ruzbahman, M. Predicting wheat production in Iran using an artificial neural networks approach. *Int. J. Acad. Res. Bus. Soc. Sci.* **2012**, *2*, 34–47.
42. Naderloo, L.; Alimardani, R.; Omid, M.; Sarmadian, F.; Javadikia, P.; Torabi, M.Y.; Alimardani, F. Application of ANFIS to predict crop yield based on different energy inputs. *Measurements* **2012**, *45*, 1406–1413. [CrossRef]
43. Khashei-Siuki, A.; Kouchakzadeh, M.; Ghahraman, B. Predicting dryland wheat yield from meteorological data, using expert system, Khorasan Province, Iran. *J. Agric. Sci. Tech-Iran* **2011**, *13*, 627–640.
44. Alvarez, R. Predicting average regional yield and production of wheat in the Argentine Pampas by an artificial neural network approach. *Eur. J. Agron.* **2009**, *30*, 70–77. [CrossRef]
45. Hill, B.D.; McGinn, S.M.; Korchinski, A.; Burnett, B. Neural network models to predict the maturity of spring wheat in western Canada. *Can. J. Plant Sci.* **2002**, *82*, 7–13. [CrossRef]
46. Zhang, H.; Hu, H.; Zhang, X.; Zhu, L.; Zheng, K.; Jin, Q.; Zeng, F. Estimation of rice neck blasts severity using spectral reflectance based on BP-neural network. *Acta Physiol. Plant.* **2011**, *33*, 2461–2466. [CrossRef]
47. Ji, B.; Sun, Y.; Yang, S.; Wan, J. Artificial neural networks for rice yield prediction in mountainous regions. *J. Agric. Sci.* **2007**, *145*, 249–261. [CrossRef]
48. Chen, C.; Mcnairn, H. A neural network integrated approach for rice crop monitoring. *Int. J. Remote Sens.* **2006**, *27*, 1367–1393. [CrossRef]
49. Chantre, G.R.; Blanco, A.M.; Forcella, F.; van Acker, R.C.; Sabbatini, M.R.; Gonzalez-Andular, J.L. A comparative study between non-linear regression and artificial neural network approaches for modelling wild oat (*Avena fatua*) field emergence. *J. Agric. Sci.* **2014**, *152*, 254–262. [CrossRef]
50. Chayjan, R.A.; Esna-Ashari, M. Modeling of heat and entropy sorption of maize (cv. Sc704): Neural network method. *Res. Agric. Eng.* **2010**, *56*, 69–76. [CrossRef]

51. O'Neal, M.R.; Engel, B.A.; Ess, D.R.; Frankenberger, J.R. Neural network prediction of maize yield using alternative data coding algorithms. *Biosyst. Eng.* **2002**, *83*, 31–45.
52. Matsumura, K.; Gaitan, C.F.; Sugimoto, K.; Cannon, A.J.; Hsieh, W.W. Maize yield forecasting by linear regression and artificial neural networks in Jilin, China. *J. Agric. Sci.* **2014**, *153*, 399–410. [CrossRef]
53. Morteza, T.; Asghar, M.; Hassan, G.M.; Hossein, R. Energy consumption and modeling of output energy with multilayer feed-forward neural network for corn silage in Iran. *Agric. Eng. Int. CIGR J.* **2012**, *14*, 93–101.
54. Uno, Y.; Prasher, S.; Lacroix, R.; Goel, P.; Karimi, Y.; Viau, A.; Patel, R. Artificial neural networks to predict corn yield from compact airborne spectrographic imager data. *Comput. Electron. Agric.* **2005**, *47*, 149–161. [CrossRef]
55. Kaul, M.; Hill, R.L.; Walthall, C. Artificial neural networks for corn and soybean yield prediction. *Agric. Syst.* **2005**, *85*, 1–18. [CrossRef]
56. Chayjan, R.A.; Esna-Ashari, M. Modeling Isosteric Heat of Soya Bean for Desorption Energy Estimation Using Neural Network Approach. *Chil. J. Agric. Res.* **2010**, *70*, 616–625. [CrossRef]
57. Higgins, A.; Prestwidge Di Tirling, S.D.; Yost, J. Forecasting maturity of green peas: An application of neural networks. *Comput. Electron. Agric.* **2010**, *70*, 151–156. [CrossRef]
58. Vázquez-Rueda, M.G.; Ibarra-Reyes, M.; Flores-García, F.G.; Moreno-Casillas, H.A. Redes neuronales aplicadas al control de riego usando instrumentación y análisis de imágenes para un microinvernadero aplicado al cultivo de Albahaca. *Res. Comput. Sci.* **2018**, *147*, 93–103.
59. Zhang, W.; Bai, X.; Liu, G. Neural network modeling of ecosystems: A case study on cabbage growth system. *Ecol. Model.* **2007**, *201*, 317–325. [CrossRef]
60. Stastny, J.; Konecny, V.; Trenz, O. Agricultural data prediction by means of neural networks. *Agric. Econ. Czech* **2011**, *57*, 356–361.
61. Fortin, J.G.; Anctil, F.; Parent, L.E.; Bolinder, M.A. A neural network experiment on the site-specific simulation of potato tuber growth in Eastern Canada. *Comput. Electron. Agric.* **2010**, *73*, 126–132. [CrossRef]
62. Fortin, J.G.; Anctil, F.; Parent, L.E.; Bolinder, M.A. Site-specific early season potato yield forecast by neural network in Eastern Canada. *Precis. Agric.* **2010**, *12*, 905–923. [CrossRef]
63. Naroui Rad, M.R.; Koohkan, S.; Fanaei, H.R.; Pahlavan Rad, M.R. Application of Artificial Neural Networks to predict the final fruit weight and random forest to select important variables in native population of melon (*Cucumis melo* L.). *Sci. Hortic.* **2015**, *181*, 108–112. [CrossRef]
64. Pascual-Sánchez, I.A.; Ortiz-Díaz, A.A.; Ramírez-de la Rivera, J.; Figueredo-León, A. Predicción del Rendimiento y la Calidad de Tres Gramíneas en el Valle del Cauto. *Rev. Cuba. Cienc. Inf.* **2017**, *11*, 144–158.
65. Lobato-Fernandes, J.; Favilla Ebecken, N.F.; dalla Mora-Esquerdo, J.C. Sugarcane yield prediction in Brazil using NDVI time series and neural networks ensemble. *Int. J. Remote Sens.* **2017**, *38*, 4631–4644. [CrossRef]
66. Vásquez, V.; Lescano, C. Predicción por Redes Neuronales Artificiales de la Calidad Fisicoquímica de Vinagre de Melaza de Caña por Efecto de Tiempo-Temperatura de Alimentación a un Evaporador Destilador-Flash. *Sci. Agropecu.* **2010**, *1*, 63–73. [CrossRef]
67. Soares, J.; Pasqual, M.; Lacerda, W.; Silva, S.; Donato, S. Utilization of Artificial Neural Networks in the Prediction of the Bunches' Weight in Banana Plants. *Sci. Hortic.* **2013**, *155*, 24–29. [CrossRef]
68. Ávila-de Hernández, R.; Rodríguez-Pérez, V.; Hernández-Caraballo, E. Predicción del Rendimiento de un Cultivo de Plátano mediante Redes Neuronales Artificiales de Regresión Generalizada. *Publ. Cienc. Tecnol.* **2012**, *6*, 31–40.
69. Hernández-Caraballo, E.A. Predicción del Rendimiento de un Cultivo de Naranja "Valencia" Mediante Redes Neuronales de Regresión Generalizada. *Publ. Cienc. Tecnol.* **2015**, *9*, 139–158.
70. Rojas-Naccha, J.; Vásquez-Villalobos, V. Prediction by Artificial Neural Networks (ANN) of the Diffusivity, Mass, Moisture, Volume and Solids on Osmotically Dehydrated Yacon (*Smallantus sonchifolius*). *Sci. Agropecu.* **2012**, *3*, 201–214. [CrossRef]
71. Bala, B.; Ashraf, M.; Uddin, M.; Janjai, S. Experimental and Neural Network Prediction of the Performance of a Solar Tunnel Drier for a Solar Drying Jack Fruit Bulbs and Leather. *J. Food Process. Eng.* **2005**, *28*, 552–566. [CrossRef]
72. Hernández-Caraballo, E.A.; Avila, G.R.; Rivas, F. Las Redes Neuronales Artificiales en Química Analítica. Parte I. Fundamentos. *Rev. Soc. Venez. Quim.* **2003**, *26*, 17–25.
73. Steiner, A.A. A Universal Method for Preparing Nutrient Solutions of a Certain Desired Composition. *Plant Soil* **1961**, *15*, 134–154. [CrossRef]

74. Trudgill, D.L.; Honek, A.; Li, D.; van Straalen, N.M. Thermal time—Concepts and utility. *Ann. Appl. Biol.* **2005**, *146*, 1–14. [CrossRef]
75. Ardila, G.; Fischer, G.; Balaguera, H. Caracterización del Crecimiento del Fruto y Producción de Tres Híbridos de Tomate (*Solanum lycopersicum* L.) en Tiempo Fisiológico bajo Invernadero. *Rev. Colomb. Cienc. Hortic.* **2011**, *5*, 44–56. [CrossRef]
76. Goudriaan, J.; van Laar, H.H. *Modelling Potential Crop Growth Processes*; Kluwer Academic Publishers: Dordrecht, The Netherlands, 1994; p. 239.
77. Hunter, D.; Yu, H.; Pukish, M.; Kolbusz, J.; Wilamowski, B. Selection of Proper Neural Network Sizes and Architectures—A Comparative Study. *IEEE Trans. Ind. Inf.* **2012**, *8*, 228–240. [CrossRef]
78. Marquardt, D.W. An algorithm for least-squares estimation of nonlinear parameters. *J. Soc. Ind. Appl. Math.* **1963**, *11*, 431–441. [CrossRef]
79. Levenberg, K. A method for the solution of certain nonlinear problems in least squares. *Q. Appl. Math.* **1944**, *2*, 164–168. [CrossRef]
80. Jain, Y.K.; Bhandare, S.K. Min Max Normalization Based Data Perturbation Method for Privacy Protection. *Int. J. Comput. Commun. Technol.* **2011**, *2*, 45–50.
81. Han, J.; Kamber, M. *Data Mining—Concepts and Techniques*, 2nd ed.; Morgan Kaufmann Publishers: Massachusetts, USA, 2006.
82. R Core Team. *R: A Language and Environment for Statistical Computing. R Foundation for Statistical Computing*; Andy Bunn and Mikko Korpela: Vienna, Austria, 2015; Available online: https://www.R-project.org (accessed on 11 February 2018).
83. Xu, Y.; Goodacre, R. On Splitting Training and Validation Set: A Comparative Study of Cross-Validation, Bootstrap and Systematic Sampling for Estimating the Generalization Performance of Supervised Learning. *J. Anal. Test.* **2018**, *2*, 249–262. [CrossRef]
84. Esen, H.; Inalli, M.; Sengur, A.; Esen, M. Forecasting of a ground-coupled heat pump performance using neural networks with statistical data weighting pre-processing. *Int. J. Therm. Sci.* **2008**, *47*, 431–441. [CrossRef]
85. Demuth, H.B.; Beale, M.H. *Neural Network Toolbox for Use with Matlab: User's Guide*; MathWorks: Pennsylvania, USA, 2001.
86. Demuth, H.B.; Beale, M.H.; De Jesús, O.; Hagan, M.T. *Neural Network Design*, 2nd ed.; Hagan: Stillwater, OK, USA, 2014.
87. Tohidi, M.; Sadeghi, M.; Mousavi, S.R.; Mireei, S.A. Artificial neural network modeling of process and product indices in deep bed drying of rough rice. *Turk. J. Agric. For.* **2012**, *36*, 738–748.
88. Dorofki, M.; Elshafie, A.H.; Jaafar, O.; Karim, O.A.; Mastura, S. Comparison of Artificial Neural Network Transfer Functions Abilities to Simulate Extreme Runoff Data. In Proceedings of the 2012 International Conference on Environment, Energy and Biotechnology, Kuala Lumpur, Malaysia, 5–6 May 2012.
89. Obe, O.O.; Shangodoyin, D.K. Artificial neural network based model for forecasting sugar cane production. *J. Comput. Sci.* **2010**, *6*, 439–445.
90. Gutiérrez, H.; De La Vara, R. *Análisis y Diseños de Experimentos*; McGraw-Hill Interamericana: Mexico, 2003; p. 430.
91. Chandwani, V.; Agrawal, V.; Nagar, R.; Singh, S. Modeling slump of ready mix concrete using artificial neural network. *Int. J. Technol.* **2015**, *6*, 207–216. [CrossRef]
92. Ljung, L. Perspectives on system identification. In Proceedings of the 17th IFAC World Congress, Seoul, Korea, 6–11 July 2008; pp. 7172–7184.
93. Ochoa-Martínez, C.I.; Ramaswamy, H.S.; Ayala-Aponte, A.A. Artificial Neural Network modeling of osmotic dehydration mass transfer kinetics of fruits. *Dry. Technol.* **2007**, *25*, 85–95. [CrossRef]
94. Vargas-Sállago, J.M.; López-Cruz, I.L.; Rico-García, E. Redes neuronales artificiales aplicadas a mediciones de fitomonitoreo para simular fotosíntesis en jitomate bajo invernadero. *Rev. Mex. Cienc. Agríc.* **2012**, *4*, 747–756.
95. Arahal, M.R.; Soria, M.B.; Díaz, F.R. *Técnicas de Predicción con Aplicaciones en Ingeniería*; Universidad de Sevilla: Sevilla, Spain, 2006; p. 340.
96. Millan, F.R.; Ostojich, Z. Predicción mediante redes neuronales artificiales de la transferencia de masa en frutas osmóticamente deshidratadas. *Interciencia* **2006**, *31*, 206–210.

97. Chen, C.R.; Ramaswamy, H.S.; Alli, I. Prediction of quality changes during osmo-convective drying of blueberries using neural network models for process optimization. *Dry. Technol.* **2001**, *19*, 515. [CrossRef]
98. Martín, Q.; De Paz, Y.R. *Aplicación de las Redes Neuronales Artificiales a la Regresión*; La Muralla: Madrid, Spain, 2007; p. 52.
99. Isasi, P.; Galván, I.M. *Redes Neuronales Artificiales. Un Enfoque Práctico*; Pearson Educación: Madrid, Spain, 2004; p. 90.